THIRD EUROPEAN ROTORCRAFT AND POWERED LIFT AIRCRAFT FORUM

PAPER NO 16

STABILITY OF A HELICOPTER CARRYING AN UNDERSLUNG LOAD .

A PRABHAKAR *

ROYAL MILITARY COLLEGE OF SCIENCE,
SHRIVENHAM, SWINDON, UNITED KINGDOM

*(Now at Hunting Engineering, Ampthill,
Bedford)

September 7-9, 1977

AIX-EN-PROVENCE, FRANCE

ASSOCIATION AERONAUTIQUE ET ASTRONAUTIQUE DE FRANCE

STABILITY OF A HELICOPTER CARRYING AN UNDERSLUNG LOAD

A PRABHAKAR *

Royal Military College of Science, Shrivenham, Swindon
United Kingdom

1. INTRODUCTION

Applications of helicopters have included their uses as aerial cranes and for transporting awkward loads by slinging externally beneath the fuselage. Normal operating speeds of modern helicopters are uprated continuously, but when carrying loads externally the forward speed is severely restricted, sometimes by the power and control limitations of the helicopter itself, but more usually because of the onset of dynamic instability of the load. This has directed increasing attention to the problems of carrying loads externally.

The earliest underslung loads were carried by a single point suspension; theoretical investigations of a hovering helicopter with a load suspended from a fixed hook were published by Lucassen and Sterk[1] in 1965. Wolkovitch, et al [2,3] studied the dynamic stability of a helicopter carrying an underslung load, with emphasis on automatic control and stabilisation of the helicopter. These theoretical developments were also accompanied by flight tests[4-7]. It was observed in these early experiments that the commonest instability was a yawing motion of the slung load. The next logical step was therefore to provide a restraint for yaw of the load. Drogues and chutes proved to be unsatisfactory. The most successful approach has been suspension of the load from two or more points on the helicopter; consequently multipoint suspension systems are mentioned increasingly[8-12]. Surveys of the use of helicopters to carry loads externally are given in references 13 and 14.

Most theoretical investigations to date have ignored the aerodynamics of the load, with the exception perhaps of Poli and Cromack[15] who allowed for the steady aerodynamic reactions of the load (lift, drag and pitching moment).

A comprehensive study[16] of the stability of a Sea King helicopter carrying a 1996 Kg, 6.10 x 2.44 x 2.44 m (2 ton 20 x 8 x 8 ft) standard cargo container has been carried out. The suspension arrangement was the two point longitudinal suspension; the load was slung by four 6.10 m (20 ft) cables from two longitudinally separated suspension points on the helicopter (figure 1). Aerodynamic reactions (including rate dependent derivatives) of the rectangular container were determined experimentally and have been expressed fully in the equations of motion.

NOTATION

A,B,C	Inertia of helicopter for rolling, pitching, yawing motions
A_1	Lateral cyclic applied by roll autostabiliser
a_{1s}	Rotor disc fore-and-aft perturbations
$\underline{a}_s$	Vector between helicopter cg and centre of suspension spread = $\{a_{sx}, o, a_{sz}\}$
B_1	Longitudinal cyclic pitch applied by pitch autostabiliser
b_{1s}	Lateral perturbations of rotor disc
$\underline{c}$	Vector representing single idealized cable = $\{o, o, c\}$
$F_{EX,Y,Z}$	External forces acting along reference x, y, z axes
$F_{v, \text{ etc}}$	Lateral stability derivatives of rotor disc
$\underline{F}$	Force Vector
g	Gravitational constant
k	Ratio between β_2 and ρ_2 $(= \beta_2/\rho_2)$
ℓ_o	Cable length
L,M,N	Rolling, pitching and yawing moments (see below for subscripts used)

*Now at Hunting Engineering
Ampthill, Bedford.

$M_{fu,\ etc}$	Rotor disc longitudinal stability derivatives
$\underline{M}$	Moment Vector
m_H	Mass of helicopter
m_L	Mass of load
p,q,r	Helicopter roll, pitch, yaw rate
$\underline{R}$	Position vector of an elementary particle
$\underline{r}_L$	Load position vector in terms of load axes $= \{x_L, y_L, z_L\}$
s	Suspension semi-spread
U_o,u	Steady state, perturbation velocity along helicopter x-axis
V	Airspeed
$\underline{V}$	Velocity vector
$\underline{V}_O$	Velocity of origin of reference axes
v	Perturbation in sideslip velocity of helicopter
W_o,w	Steady state, perturbation velocity along helicopter z-axis
X,Y,Z	Forces along reference x,y,z axes
β_o	Steady angle made by load with helicopter x-axis
β_2	Load pitch perturbation
Θ	Angle made by helicopter x-axis with the horizontal
$\phi\ \theta\ \psi$	Rotations about helicopter x,y,z axes
θ_t	Change in tail rotor pitch
ρ	Air density
ρ_o	Steady trail angle of idealized single cable
ρ_1	Lateral angular deflection of load
ρ_2	Perturbation in cable trail angle
ρ_3	Yaw deflection of load
ω	Frequency
$\underline{\omega}$	Angular velocity of helicopter frame of reference

Subscripts:

A	Aerodynamic
E	External
G	Gravitational
H	Helicopter
I	Interaction
L	Load
u,v, etc	Helicopter stability derivatives
Lρ3, Lv, etc	Load stability derivatives

2. DERIVATION OF THE EQUATIONS OF MOTION

The helicopter-underslung load system consists essentially of two interacting bodies moving through space. To derive the equations of motion of such a system immediate simplications may be made by neglecting the structural elasticity of both the helicopter and the load, and by ignoring the mass of the cables and their aerodynamic reactions.

The helicopter may therefore be modelled as a primary body with six spatial degrees of freedom - three translational and three rotational. The underslung load may be supposed a secondary body attached to the helicopter by the suspension which allows the load to move relative to the helicopter. Assuming the suspension arrangement to be analytical, the four cables may be replaced by equations of constraint acting on the load; the forces and moments transmitted by the suspension may be represented as extra "external" interaction forces and moments acting on both the helicopter and the load. The analytical model obtained therefore is as in figure 2 of two rigid interacting bodies moving through space. Equations of motion of such a dynamic system are obtained by applying Newton's laws of motion to the helicopter and load in turn.

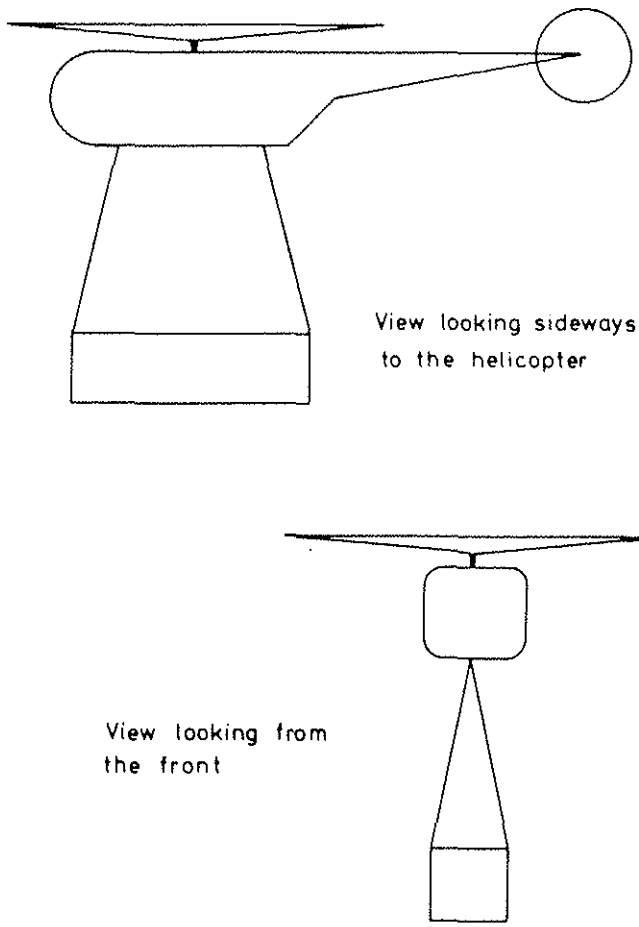

FIGURE 1 TWO POINT LONGITUDINAL SUSPENSION

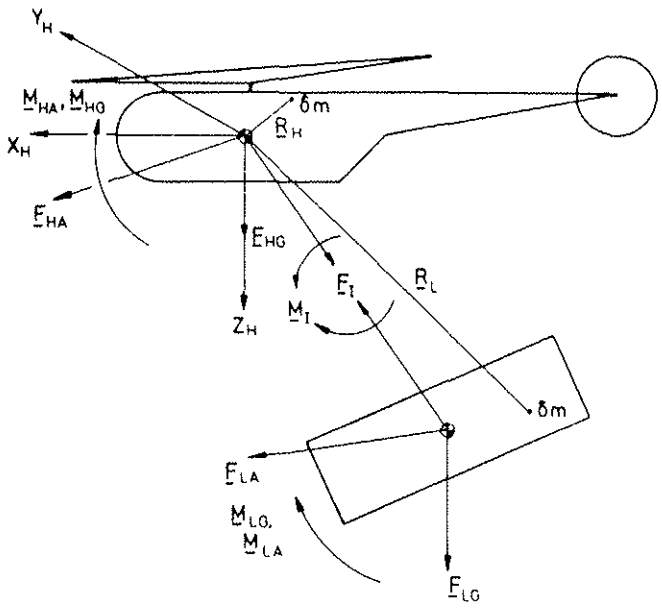

FIGURE 2 FREE BODY DIAGRAM FOR THE DERIVATION OF THE EQUATIONS OF MOTION

The vector forms of Newton's laws for a body of constant mass are [17]:

$$\text{Force Equation: } \sum \delta m \frac{d\underline{V}}{dt} = \underline{F}_E \qquad (1)$$

$$\text{Moments Equation: } \sum \delta m \, \underline{R} \wedge \frac{d\underline{V}}{dt} = \underline{M}_E \qquad (2)$$

Equations are derived relative to a moving frame of axes (X_H Y_H Z_H in figure 2) fixed at the helicopter centre of mass.

2.1 Derivation of the Helicopter Equations

If the helicopter is assumed to be a rigid body the position vector for an elementary particle δm of the helicopter is a constant. External forces and moments on the helicopter are defined in the free body diagram (figure 2). If $\underline{V}_0$ is the translational velocity and $\underline{\omega}$ the angular velocity of the helicopter frame of reference then the velocity of an element of the helicopter is given by

$$\underline{V}_H = \underline{V}_0 + \underline{\omega} \wedge \underline{R}_H \qquad (3)$$

Making use of (3) and (1) and summing over the helicopter the force equation is obtaine as:

$$m_H (\dot{\underline{V}}_0 + \dot{\underline{\omega}} \wedge \underline{V}_0) = \underline{F}_{HA} + \underline{F}_{HG} + \underline{F}_I \qquad (4)$$

Similarly using equations 3 and 2 gives the helicopter moments equation as:

$$\sum_H \delta m \, (\dot{\underline{\omega}} R_H^2 - \underline{R}_H \dot{\underline{\omega}} \cdot \underline{R}_H + \underline{R}_H \wedge \underline{\omega} \, \underline{R}_H \cdot \underline{\omega}) = \underline{M}_{HA} + \underline{M}_{HG} + \underline{M}_I \qquad (5)$$

2.2 Derivation of the Load Equations of Motion

External forces and moments acting on the load are shown in figure 2; the interactive forces and moments acting on the load are equal and opposite to those acting on the helicopter.

Because of the relative motion between helicopter and load, $\underline{R}_L$ the position of an element of the load is a variable; the velocity of δm in space is therefore

$$\underline{V}_L = \underline{V}_0 + \dot{\underline{R}}_L + \underline{\omega} \wedge \underline{R}_L$$

$$\text{and } \frac{d\underline{V}_L}{dt} = \dot{\underline{V}}_0 + \ddot{\underline{R}}_L + \dot{\underline{\omega}} \wedge \underline{R}_L + 2\underline{\omega} \wedge \dot{\underline{R}}_L + \underline{\omega} \wedge \underline{V}_0 + \underline{\omega} \wedge (\underline{\omega} \wedge \underline{R}_L) \qquad (6)$$

Using (6) in equation (1) and simplifying gives the force equation for the load:

$$m_L (\dot{\underline{V}}_0 + \underline{\omega} \wedge \underline{V}_0) + \sum_L \delta m \left[\ddot{\underline{R}}_L + \dot{\underline{\omega}} \wedge \underline{R}_L + 2\underline{\omega} \wedge \dot{\underline{R}}_L + \underline{\omega} \wedge (\underline{\omega} \wedge \underline{R}_L) \right] \qquad (7)$$

$$= \underline{F}_{LA} + \underline{F}_{LG} - \underline{F}_I$$

Similarly the moments equation for the load is obtained as

$$\sum_L \delta m \left[\underline{R}_L \wedge \dot{\underline{V}}_0 + \underline{R}_L \wedge \ddot{\underline{R}}_L + \dot{\underline{\omega}} R_L^2 - \underline{R}_L \dot{\underline{\omega}} \cdot \underline{R}_L + 2\underline{\omega}\, \underline{R}_L \cdot \dot{\underline{R}}_L \right.$$

$$\left. - (2\dot{\underline{R}}_L + \underline{V}_0)\, \underline{\omega} \cdot \underline{R}_L + \underline{\omega}\, \underline{V}_0 \cdot \underline{R}_L + \underline{R}_L \wedge \underline{\omega}\, \underline{R}_L \cdot \omega \right] \qquad (8)$$

$$= \underline{M}_{LA} + \underline{M}_{LG} - \underline{M}_I$$

The four vector equations of motion above (equations 4,5,7,8) describe the motion of two interacting, rigid bodies moving through space. These equations are referred to axes fixed at the centre of mass of the primary body (helicopter) and are quite general; they can be applied to any particular problem by a suitable definition of $\underline{R}_L$, $\underline{F}_I$, $\underline{M}_I$. For the helicopter-underslung load case this requires a thorough analysis of the suspension arrangement.

2.3 Definition of Load Position Vector $\underline{R}_L$

The load position vector $\underline{R}_L$ in the equations of motion above can be conveniently represented as a sum of constant and variable terms such that, with reference to figure 3,

$$\underline{R}_L = \underline{a}_s + \underline{c}_H + \underline{r}_{LH}$$

A convenient point O_s is taken on the helicopter and $\underline{a}_s$ is the distance between G, the origin of the helicopter axes, and O_s; this distance is constant for a rigid helicopter.

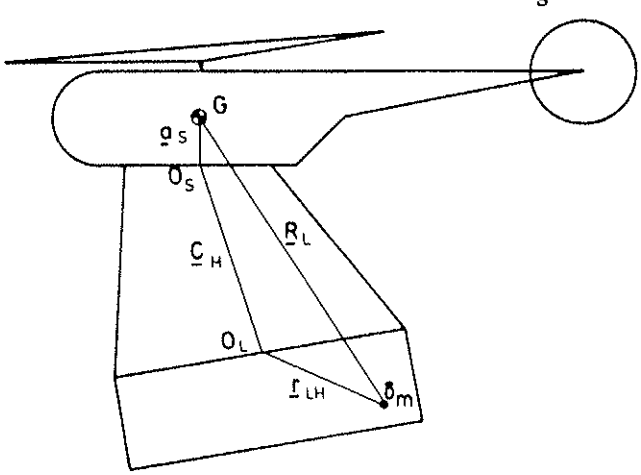

FIGURE 3 DEFINITION OF LOAD POSITION VECTOR $\underline{R}_L$

Another convenient point O_L is taken on the load. The distance $\underline{c}_H$ between the helicopter and load is given by the line $O_s O_L$, and the distance from O_L to an elementary load particle δm by $\underline{r}_{LH}$. Both $\underline{c}_H$ and $\underline{r}_{LH}$ are allowed to vary with time in the helicopter frame of reference in a manner governed by the suspension arrangement

Further simplifications may be made by defining two secondary sets of axes:

(i) A cable frame of reference, with origin at O_s and moving as the vector $\underline{c}_H$ moves relative to the helicopter.

(ii) A load frame of reference, origin at O_L, and moving with the load.

Advantage of defining these axes is that both the suspension and load vectors may be taken to be constants in their respective frames of reference. They may be referred to the helicopter axes by suitable time variant transformation matrices which specify motion relative to the helicopter frame of reference. If T_C and T_L are these transformation matrices then

$$\underline{R}_L = \underline{a}_s + T_C \underline{c} + T_L \underline{r}_L \qquad (9)$$

where $\underline{c}$ and $\underline{r}_L$ are constant vectors defined in the suspension and load frames of reference respectively.

3. ANALYSIS OF SUSPENSION

The suspension arrangement is inherently non-linear, and analysis can only be carried out after making simplifying assumptions:

(i) The cables do not support compressive forces and are in tension

(ii) Cables are inextensible

(iii) There is no aerodynamic loading on the cables

(iv) Helicopter attitude is horizontal

Observations on a slung model of the load show three major degrees of freedom.

(i) fore and aft (pitch) oscillation

(ii) sideways oscillation, also termed the lateral pendulum

(iii) a yawing oscillation.

3.1 Longitudinal Analysis

For four equal length suspension cables a plane of symmetry is formed; the suspension can then be represented by two cables in this plane of symmetry. A geometrical diagram representing the fore-and-aft motion of the load is given in figure 4. Cable length in the plane of symmetry is

$$\ell' = \sqrt{\ell_o^2 - Y^2} \qquad (10)$$

Initial position of the load hanging vertically beneath the helicopter is shown by the dotted lines in figure 4. As the helicopter commences forward flight the load trails back to another equilibrium position, shown by the solid lines.

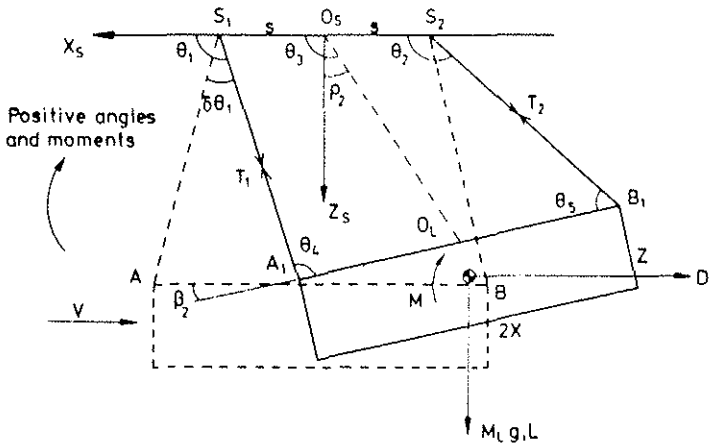

FIGURE 4 SKETCH OF LOAD AND SUSPENSION IN THE PLANE OF SYMMETRY

Kinematic Analysis

If the cables are assumed to be inextensible and undeformed by any aerodynamic loading then the ends of the two virtual cables in the plane of symmetry describe circles of radii ℓ, and distance between them is equal to the load length 2X. Hence from simple geometrical properties the relationship between the trail angles θ_1, θ_2 of the front and rear cables respectively is obtained as

$$2s\ell(\cos\theta_1 - \cos\theta_2) + \ell^2 \left[1 - \cos(\theta_1 - \theta_2) \right] = 2(X^2 - s^2) \qquad (11)$$

This equation may be solved numerically for θ_2, assuming known values of θ_1. The angle of rotation of load is then given by

$$\beta_2 = \sin^{-1} \frac{\ell}{2X} (\sin\theta_1 - \sin\theta_2) \qquad (12)$$

From the two cable simplification the suspension may further be reduced to a single idealized cable joining the mid-points of the suspension spread and of the top surface of the load. This was shown to be convenient in the definition of load position vector $\underline{R}_L$ (Section 2.3 above). The angle made by this single idealized cable is found to be

$$\theta_3 = \tan^{-1} \frac{\sin\theta_1 + \sin\theta_2}{\cos\theta_1 + \cos\theta_2} \qquad (13)$$

and the length is obtained as

$$c = \frac{\ell}{2} \sqrt{2 + 2 \cos (\theta_1 - \theta_2)} \qquad (14)$$

The variation of the above quantities as the trail angle of the front cable is increased as shown in figure 5 for a suspension spread of 4.57m (15 ft). It is seen that despite the non-linear relationships obtained above, the graphs are remarkably linear over the range considered.

If the trail angle of the idealized cable is defined as

$$\rho_2 = 90^\circ - \theta_3 \qquad (15)$$

and this quantity plotted against β_2, the angle made by the load, a linear plot is obtained of slope 0.255 for a 4.57m (15 ft) spread. Load rotation can thus be simply expressed in terms of the trail angle of the single idealized cable in the plane of symmetry.

Steady State Longitudinal Aerodynamics

As equations of motion are generally derived for perturbations from an equilibrium position it is necessary to determine the equilibrium position of the load relative to the helicopter. The easiest approach is to assume a load trail angle and obtain the kinematics of the suspension for that configuration. By equating the load aerodynamic reactions 15,18 to the cable tensions for equilibrium the airspeed which would cause the load to trail to that position can be calculated.

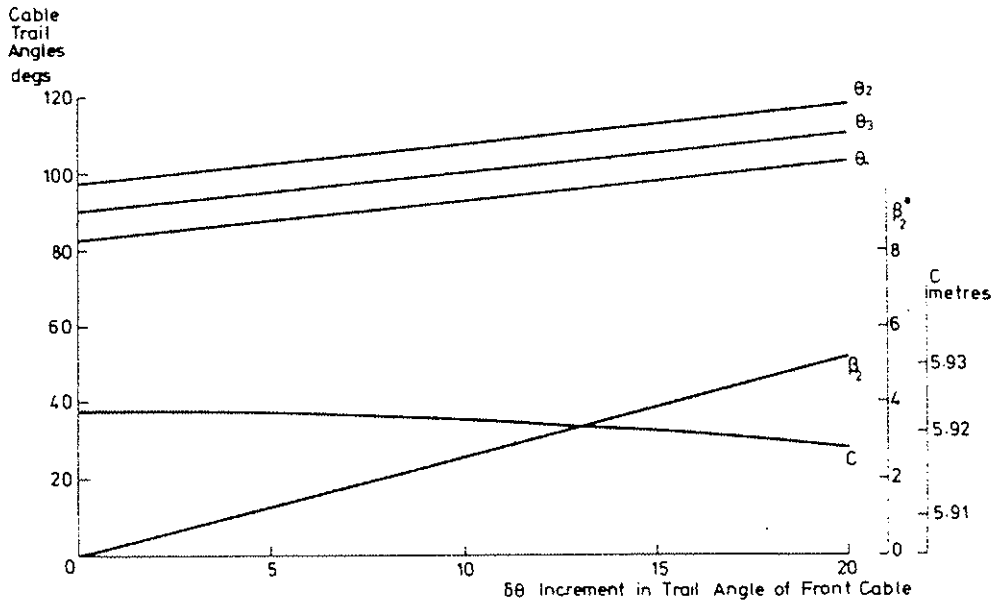

FIGURE 5 RESULTS OF LONGITUDINAL GEOMETRICAL ANALYSIS
4.57m (15ft) SUSPENSION SPREAD

Results obtained for the load aerodynamic data from Poli and Cromack [15] are shown in figure 6 for a 4.57 m suspension spread.

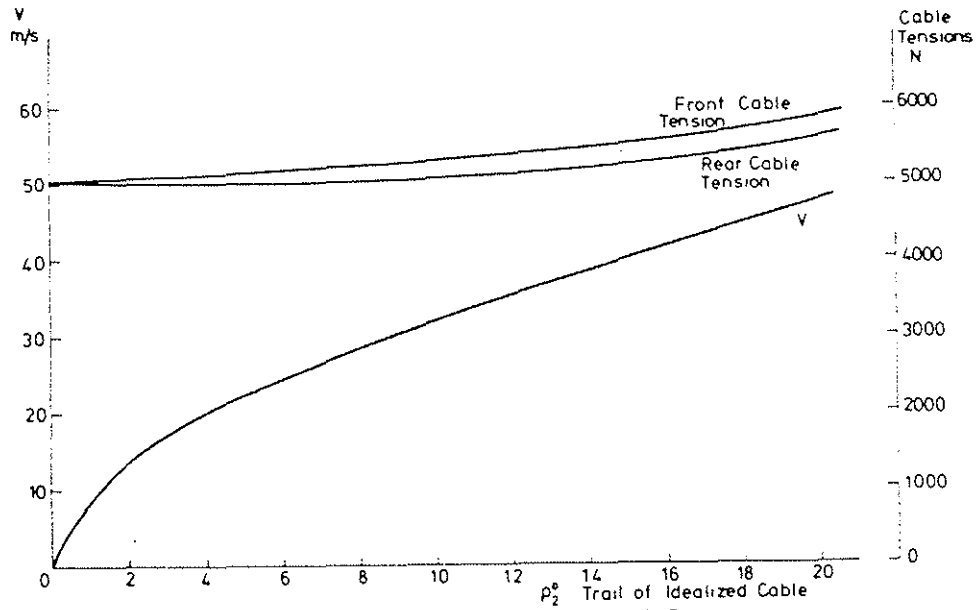

FIGURE 6 VARIATION OF AIRSPEED AND CABLE TENSIONS FOR 4.57m (15ft) SUSPENSION SPREAD

3.2 Lateral Analysis

The load lateral motion is that of load swinging side-to-side without taking up a steady lateral position, and is a purely dynamic phenomenon. The lateral analysis therefore consists essentially of verifying that the single cable representation obtained in the last section is also valid for the lateral mode. Lateral aerodynamic effects manifest themselves by an induced sideslip velocity and are allowed for in the stability derivatives for the equations of motion.

3.3 Yaw Analysis

If it is assumed that the suspension cables are in tension, then the constraints imposed by four cables in tension remove four of the six spatial degrees of freedom of the load leaving it with only the longitudinal and lateral degrees of freedom. The third degree of freedom of the load - yawing oscillation - therefore must violate at least one of the constraints imposed by the idealized suspension and shows the major difficulty in attempting to represent the suspension analytically.

If a model of the load, hanging vertically below the helicopter, is yawed it is seen that after a sufficiently large deflection the load is supported by only two diagonally opposed cables, the other two being slack. The point at which two cables become slack is a function of the cable flexibility; for the assumed suspension of inflexible cables this would take place for an infinitesimal deflection from the zero yaw condition. This change of state of the system, from all four cables in tension to two going slack, is a serious non-linearity of the assumed suspension. If two of the cables go slack then another degree of freedom about the axis formed by the two cables in tension is possible. This was however ignored.

Another problem is the correct definition of load yaw. The yawing axis is self-evident at hover but not so obvious when the load trails back during forward flight. This problem is discussed fully elsewhere [16]; the definition of load yaw adopted was as a rotation about the load z-axis.

Because of the inherent difficulties and the lengthy mathematics involved [16] only the results from yaw analysis are discussed here.

Moment required to displace the underslung load through a yaw angle of ρ_3 can be calculated from a knowledge of suspension and load parameters. This moment may be considered a restoring moment tending to return the load to its zero yaw position, and is the yawing restraint imposed on the load by the two point longitudinal suspension.

The yaw restoring moments at hover for a range of cable flexibilities are plotted in figure 7 for a suspension spread of 4.57m (15 ft). It is seen that inflexible cables give a yaw restoring moment even for zero yaw because of the suspension non-linearity. With flexible cables there is a gradual increase in yawing moment from zero yaw; these graphs however show a discontinuity at certain values of yaw angle where two of the cables become slack and the load weight is supported by two flexible cables only.

Thus by introducing the flexibility of cables suspension properties are changed such that the suspension system becomes linear for a range of angles about the zero yaw position of the load. This linear relationship is however only valid up to the angle at which two of the cables become slack.

Yaw analysis for the load at a steady trail angle is a very complex three dimensional problem. The conclusion reached as a result of this analysis was that the yawing restraint of the suspension arrangement at a steady trail angle could be adequately represented by the results obtained from the hover analysis.

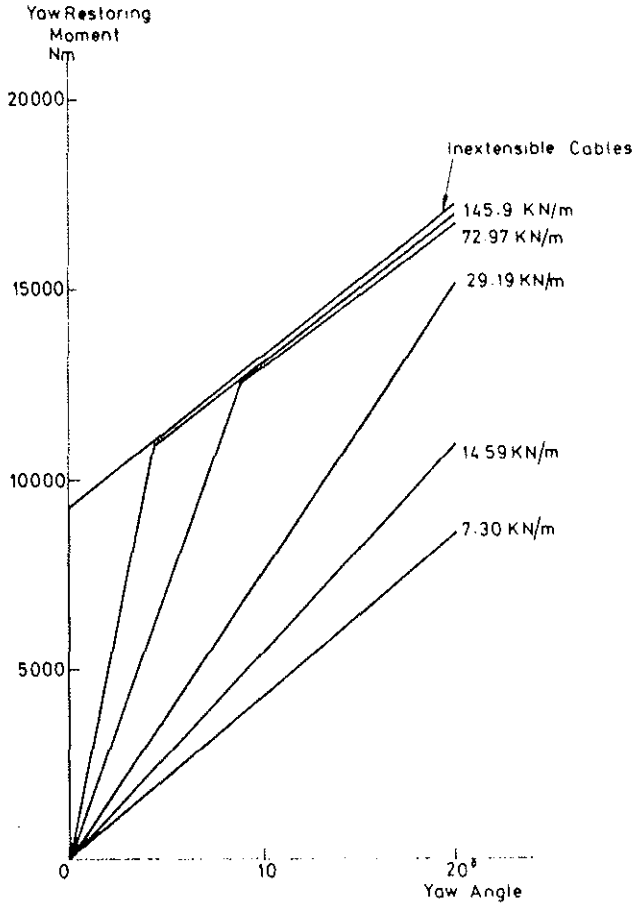

FIGURE 7 YAW RESTORING MOMENT AT HOVER 4.57m(15ft) SUSPENSION SPREAD

4. SCALAR EQUATIONS OF MOTION

The four vector equations derived earlier (equations 4, 5, 7, 8) are equivalent to 12 scalar equations of motion. The helicopter-underslung load system however has only nine degrees of freedom - six for the helicopter and three for the load (mentioned in section 3). This redundance of equations can be resolved simply by adding the helicopter and load force equations, giving a combined force equation:

$$(m_H + m_L)\ (\dot{\underline{V}}_0 + \underline{\omega} \wedge \underline{V}_0) + \sum_L \delta m \left[\ddot{\underline{R}}_L + \dot{\underline{\omega}} \wedge \underline{R}_L + 2\underline{\omega} \wedge \dot{\underline{R}}_L + \underline{\omega} \wedge (\underline{\omega} \wedge \underline{R}_L)\right] \tag{16}$$

$$= \underline{F}_{HA} + \underline{F}_{LA} + \underline{F}_{HG} + \underline{F}_{LG}$$

Equation 16, and the two moment equations 5, 8, are sufficient to describe the dynamics of the system formed by a helicopter carrying an underslung load. These equations must be obtained in terms of their scalar components.

A major unknown in the equations of motion is the load position vector $\underline{R}_L$. Two transformation matrices (equation 9) are required to yield scalar components of $\underline{R}_L$; these matrices can be derived from the sequence of rotations which take the load to its perturbed position [19].

The idealized single cable executes only two motions: trail angle ρ_{20} and lateral motion ρ_1. The load can undergo three rotations: β_{20} in the longitudinal plane, lateral motion ρ_1, and load yaw ρ_3 about the load z axis. The derivation of these transformation matrices is shown in detail in the author's PhD thesis [16].

Two further assumptions can be reasonably made:

(i) Suspension points are in the plane of symmetry of the helicopter, with their mid-point vertically below the helicopter reference.

(ii) The single idealized cable of length c (given by equation 14) is along the cable reference z axis.

ie $\underline{a}_s = \{a_{sx}, o, a_{sz}\}$ and $\underline{c} = \{o, o, c\}$

Load vector can be written as $\underline{r}_L = \{x_L, y_L, z_L\}$

where the components are referred to the centre of the top surface of the load (point O_L in figure 3).

In normal flight the load would take up a steady trail angle position and then show perturbations about this position. Therefore trail angles can be written as:

$$\rho_{20} = \rho_0 + \rho_2 \quad \text{and} \quad \beta_{20} = \beta_0 + \beta_2$$

where ρ_0, β_0 are the steady state values, and ρ_2, β_2, are small perturbations, as are ρ_1, ρ_3. $\underline{R}_L$ can therefore be linearised by ignoring second and higher order terms giving:

$$\underline{R}_L = \begin{bmatrix} a_{sx} \\ 0 \\ a_{sz} \end{bmatrix} + \begin{bmatrix} \sin\rho_0 + \rho_2\cos\rho_0 \\ -\rho_1\cos\rho_0 \\ \cos\rho_0 - \rho_2\sin\rho_0 \end{bmatrix} c \qquad (17)$$

$$+ \begin{bmatrix} \cos\beta_0 - \beta_2\sin\beta_0 & -\rho_3\cos\beta_0 & \sin\beta_0 + \beta_2\cos\beta_0 \\ \rho_1\sin\beta_0 + \rho_3 & 1 & -\rho_1\cos\beta_0 \\ -\sin\beta_0 - \beta_2\cos\beta_0 & \rho_3\sin\beta_0 + \rho_1 & \cos\beta_0 - \beta_2\sin\beta_0 \end{bmatrix} \begin{bmatrix} x_L \\ y_L \\ z_L \end{bmatrix}$$

The helicopter has a linear velocity $\underline{V}$ and an angular velocity $\underline{\omega}$.

The linear velocity components may be written as the sum of steady state and perturbation values, and the angular velocity is assumed to be small perturbations ie

$$\underline{V}_0 = \underline{i}\,(U_o + u) + \underline{j}\,(V_o + v) + \underline{k}\,(W_o + w) \qquad (18)$$

$$\text{and } \underline{\omega} = \underline{i}\,p + \underline{j}\,q + \underline{k}\,r \qquad (19)$$

The above relationships (17, 18, 19) will express the vector equations of motion in terms of their scalar components. These equations are linearised by ignoring terms involving second and higher order perturbation variables. Normally the helicopter would not have a steady sideslip velocity ie $V_o = 0$ in equation 18 above. The resulting equations separate into longitudinal and lateral sets, shown in figures 8 and 9. Load terms in these figures have been integrated for a uniform distribution of mass and dimensions of:

Load Length = 2X Load Width = 2Y Load Depth = Z

Coordinates of load centre of gravity (0, 0, Z_G) where $Z_G = Z/2$.

5. DETERMINATION OF EXTERNAL FORCING FUNCTIONS

External forcing functions acting on the helicopter-load system are:

(i) Gravitational forces and moments

(ii) Interactive moments

(iii) Aerodynamic forces and moments.

5.1 Gravitational Forces and Moments

Helicopter and load weights act vertically downwards under gravity so the problem essentially is to obtain the relationships between the earth and helicopter frames of reference. This is solved in most standard texts [19,20] so only the results for the components of helicopter and load weight along the helicopter frames of reference are quoted:

1) Helicopter + Load X-force Equation

$$(m_H + m_L)(\dot{u} + qW_0) + m_L\left[\ddot{\rho}_2(c\sin\rho_0 + kZ_G\cos\beta_0) + \dot{q}(a_{sz} + c\cos\rho_0 + Z_G\cos\beta_0)\right] = F_{EX}$$

2) Helicopter + Load Z-force Equation

$$(m_H + m_L)(\dot{w} - qU_0) - m_L\left[\ddot{\rho}_2(c\sin\rho_0 + kZ_G\sin\beta_0) + \dot{q}(a_{sx} + c\sin\rho_0 + Z_G\sin\beta_0)\right] = F_{EZ}$$

3) Helicopter Pitching Moment Equation

$$\dot{q}B = M_{EH}$$

4) Load Moments about Helicopter Y-axis

$$\dot{q}B_{Lq} + \dot{u}B_{Lu} + \dot{w}B_{Lw} + \ddot{\rho}_2 B_{L\ddot{\rho}_2} + qB_{Lq} = M_{EL}$$

where:

$$B_{Lq} = m_L\left[a^2_{sx} + a^2_{sz} + c^2 + \tfrac{1}{3}(X^2 + Z^2) + 2a_{sx}(c\sin\rho_0 + Z_G\sin\beta_0) + 2a_{sz}(c\cos\rho_0 + Z_G\cos\beta_0) + 2cZ_G\cos(\rho_0 - \beta_0)\right]$$

$$B_{Lu} = m_L(a_{sz} + c\cos\rho_0 + Z_G\cos\beta_0)$$

$$B_{Lw} = -m_L(a_{sx} + c\sin\rho_0 + Z_G\sin\beta_0)$$

$$B_{L\ddot{\rho}_2} = m_L(ca_{sz}\cos\rho_0 + ca_{sx}\sin\rho_0 + c^2 + cZ_G\cos(\rho_0 - \beta_0) + k\left[a_{sz}Z_G\cos\beta_0 + a_{sx}Z_G\sin\beta_0 + cZ_G\cos(\rho_0 - \beta_0) + \tfrac{1}{3}(X^2 + Z^2)\right])$$

$$B_{Lq} = m_L\left[U_0(a_{sx} + c\sin\rho_0 + Z_G\sin\beta_0) + W_0(a_{sz} + c\cos\rho_0 + Z_G\cos\beta_0)\right]$$

FIGURE 8. DERIVED LONGITUDINAL EQUATIONS OF MOTION

1) Combined Helicopter-Load Sideforce Equation

$$(m_H + m_L)(\dot{v} + rP_0 - pW_0) - m_L\left[\ddot{\rho}_1(c\cos\rho_0 + Z_G\cos\beta_0) - \dot{r}(a_{sx} + c\sin\rho_0 + Z_G\sin\beta_0) + \dot{p}(a_{sz} + c\cos\rho_0 + Z_G\cos\beta_0)\right] = F_{EY}$$

2) Helicopter Rolling Moment Equation

$$\dot{p}A - \dot{r}E = L_{EH}$$

3) Helicopter Yawing Moment Equation

$$\dot{r}C - \dot{p}I = N_{EH}$$

4) Load Moments about Helicopter X-axis

$$\dot{p}A_{Lp} + \dot{r}A_{Lr} + \dot{v}A_{Lv} + \ddot{\rho}_1 A_{L\ddot{\rho}_1} + \ddot{\rho}_3 A_{L\ddot{\rho}_3} + pA_{Lp} + rA_{Lr} = L_{EL}$$

where:

$$A_{Lp} = m_L\left[a^2_{sy} + (a_{sz} + c\cos\rho_0)^2 + \tfrac{1}{3}(Y^2 + X^2\sin^2\beta_0 + Z^2\cos^2\beta_0 + 2Z_G\cos\beta_0(a_{sz} + c\cos\rho_0)\right]$$

$$A_{Lr} = -m_L\left[(a_{sx} + c\sin\rho_0)(a_{sz} + c\cos\rho_0 + Z_G\cos\beta_0) + Z_G\sin\rho_0(a_{sz} + c\cos\rho_0) + \tfrac{1}{3}(Z^2 - X^2)\sin\beta_0\cos\beta_0\right]$$

$$A_{L\ddot{\rho}_1} = -m_L\left[\tfrac{1}{3}(X^2\sin^2\beta_0 + Y^2 + Z^2\cos^2\beta_0) + cZ_G\cos\rho_0\cos\beta_0 + (a_{sz} + c\cos\rho_0)(c\cos\rho_0 + Z_G\cos\beta_0)\right]$$

$$A_{Lv} = -m_L(a_{sz} + c\cos\rho_0 + Z_G\cos\beta_0) \quad A_{Lp} = m_L W_0(a_{sz} + c\cos\rho_0 + Z_G\cos\beta_0)$$

$$A_{L\ddot{\rho}_3} = \tfrac{1}{3}m_L(X^2 + Y^2)\sin\beta_0 \quad A_{Lr} = -m_L U_0(a_{sz} + c\cos\rho_0 + Z_G\cos\beta_0)$$

5) Load Moments about Helicopter Yawing Axis

$$\dot{r}C_{Lr} + \dot{p}C_{Lp} + \dot{v}C_{Lv} + \ddot{\rho}_1 C_{L\ddot{\rho}_1} + \ddot{\rho}_3 C_{L\ddot{\rho}_3} + pC_{Lp} + rC_{Lr} = N_{EL}$$

where:

$$C_{Lr} = m_L\left[a^2_{sx} + c^2\sin^2\rho_0 + \tfrac{1}{3}(X^2\cos^2\beta_0 + Y^2 + Z^2\sin^2\beta_0) + 2a_{sx}(c\sin\rho_0 + Z_G\sin\beta_0) + 2rZ_G\sin\rho_0\sin\beta_0\right]$$

$$C_{Lp} = -m_L\left[\tfrac{1}{3}(Z^2 - X^2)\sin\beta_0\cos\beta_0 + Z_G\cos\beta_0(a_{sx} + c\sin\rho_0) + (a_{sz} + c\cos\rho_0)(a_{sx} + c\sin\rho_0 + Z_G\sin\beta_0)\right]$$

$$C_{L\ddot{\rho}_1} = -m_L\left[c\cos\rho_0(a_{sx} + c\sin\rho_0 + Z_G\sin\beta_0) + \tfrac{1}{3}(Z^2 - X^2)\cos\beta_0\sin\beta_0 + Z_G\cos\beta_0(a_{sx} + c\sin\rho_0)\right]$$

$$C_{L\ddot{\rho}_3} = \tfrac{1}{3}m_L(X^2 + Y^2)\cos\beta_0$$

$$C_{Lp} = -m_L W_0(a_{sx} + c\sin\rho_0 + Z_G\sin\beta_0) \quad C_{Lv} = m_L(a_{sx} + c\sin\rho_0 Z_G\sin\beta_0)$$

$$C_{Lr} = -m_L U_0(a_{sx} + c\sin\rho_0 + Z_G\sin\beta_0)$$

FIGURE 9. DERIVED LATERAL EQUATIONS OF MOTION

$$X_{HG} = -m_H g\,(\sin\Theta + \theta\cos\Theta) \qquad X_{LG} = -m_L g\,(\sin\Theta + \theta\cos\Theta)$$

$$Y_{HG} = m_H g\,(\psi\sin\Theta + \phi\cos\Theta) \qquad (20) \qquad X_{LG} = m_L g\,(\psi\sin\Theta + \phi\cos\Theta) \qquad (21)$$

$$Z_{HG} = m_H g(-\theta\sin\Theta + \cos\Theta) \qquad Z_{LG} = m_L g\,(-\theta\sin\Theta + \cos\Theta)$$

As the origin of the reference axes is assumed to be at the helicopter centre of gravity there are no gravitational moments due to the helicopter weight.

The weight of the load acts through its centre of gravity. The moment due to load weight about the helicopter reference is therefore:

$$\underline{M}_{LG} = \underline{R}_G \wedge \underline{F}_{LG}$$

$\underline{R}_G$ can be obtained by substituting the load centre of gravity coordinates $(0, 0, Z_G)$ into equation 17. Components of $\underline{F}_{LG}$ have already been obtained (equation 21). Simplifying the vector product and writing

$$R_{XGO} = a_{sx} + c\sin\rho_0 + Z_G\sin\beta_0$$

and $R_{ZGO} = a_{sz} + c\cos\rho_0 + Z_G\cos\beta_0$

gives:

Moments about helicopter x-axis due to load weight

$$L_{LG} = \rho_1 L_{LG\rho 1} + \psi\, L_{LG\psi} + \phi L_{LG\phi}$$

where $L_{LG\rho 1} = -m_L g\,(c\cos\rho_0 + Z_G\cos\beta_0)\cos\Theta$

$$L_{LG\psi} = -m_L g\, R_{ZGO}\sin\Theta \qquad (22)$$

$$L_{LG\phi} = m_L g\, R_{ZGO} \cos\Theta$$

Moments about helicopter y-axis

$$M_{LG} = M_{LGO} + \theta M_{LG\theta} + \rho_2 M_{LG\rho 2}$$

where $M_{LGO} = -m_L g\,(R_{ZGO} \sin\Theta + R_{ZGO} \cos\Theta)$ (23)

$$M_{LG\theta} = -m_L g\,(R_{ZGO} \cos\Theta - R_{XGO} \sin\Theta)$$

$$M_{LG\rho 2} = -m_L g\left[c \cos(\rho_0 + \Theta) + k\, Z_G \cos(\beta_0 + \Theta)\right]$$

Moments about helicopter z-axis

$$N_{LG} = \psi N_{LG\psi} + \phi N_{LG\phi} + \rho_1 N_{LG\rho 1}$$

where $N_{LG\psi} = m_L g\, R_{XGO} \sin\Theta$ (24)

$$N_{LG\phi} = m_L g\, R_{XGO} \cos\Theta$$

$$N_{LG\rho 1} = -m_L g\,(c \cos\rho_0 + Z_G \cos\beta_0) \sin\Theta$$

5.2 Interactive Moments

Results obtained from suspension analysis are used to derive the required interaction moments.

Moments about helicopter x-axis

Analysis for lateral motion of load showed that the idealized single cable is an accurate representation. Hence from simple statics the rolling moment due to the load is obtained for small ρ_1 as

$$L_I = m_L g a_{sz} \rho_1$$

Moments about y-axis

Cable tensions in the longitudinal plane were obtained during the course of longitudinal analysis of Section 3. Moment of these cable tensions about the helicopter y-axis was calculated at different cable trail angles for:

$a_{sx} = 0$, $a_{sz} = 1.75$ m (5.75 ft), spread = 4.57 m (15 ft)

When the resulting moment was plotted against the idealized single cable trail angle, a straight line of slope 850 Nm/degree was obtained ie pitch interaction moment

$$M_I = 850\, \rho_2 \text{ Nm}$$

Moments about helicopter z-axis

The suspension analysis of Section 3.3 showed that the moment required to cause a yaw deflection of the load was linear about the zero yaw position, if cable flexibility was allowed for. Wilding[5] has obtained a stiffness of 21.89 KN/m (1500 lbf ft) for the recommended terylene cables, which give a yaw restoring moment of 635 Nm/degree for a 4.57 m suspension spread ie

$$N_I = 635\, \rho_3 \text{ Nm}$$

All the interactive moments act in a restoring sense for the load but are destabilising for the helicopter as they tend to perturb the helicopter from its equilibrium position.

5.3 Helicopter Aerodynamic Reactions

In common with fixed wing aircraft, aerodynamic reactions of helicopters are expressed as stability derivatives. These derivatives for a Sea King helicopter were obtained from the manufacturers, Westland Helicopters Ltd, and are presented in full in Reference 16.

Helicopter equations as used by Westland Helicopters contain relationships for the longitudinal and lateral rotor disc degrees of freedom, and laws for the automatic stabilising equipment. These complete helicopter equations were used for stability analysis.

5.4 Load Aerodynamic Reactions

As little information was available for the aerodynamic reactions of a rectangular container they were determined experimentally. The most important result from wind tunnel tests (described in References 16 and 21) was that there was a strong pitching moment due to load pitch rate. Variation of the pitching moment coefficient due to pitch rate, is plotted against the non-dimensionalized frequency parameter in figures 10 and 11. Positive values of $C_{m\dot{\theta}}$ are destabilising.

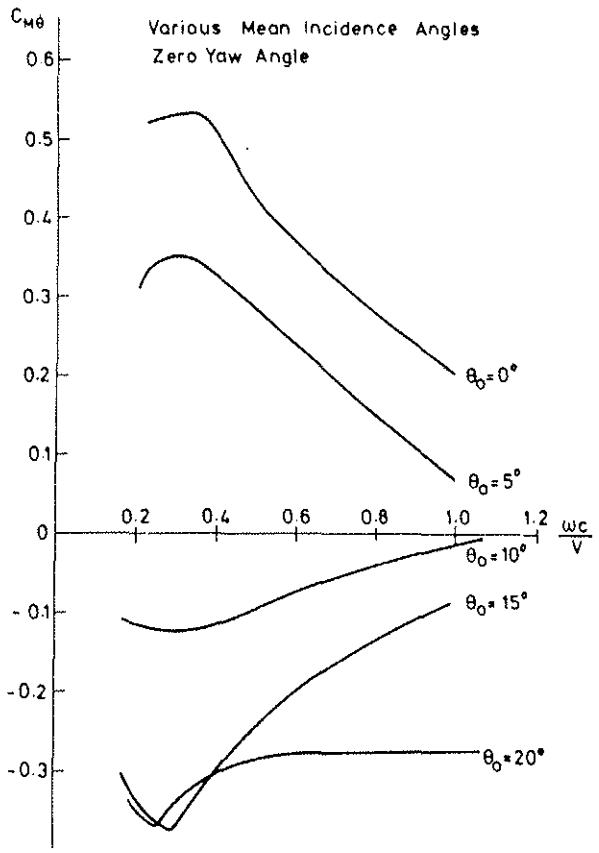

FIGURE 10 VARIATION OF $C_{M\dot{\theta}}$ WITH FREQUENCY PARAMETER

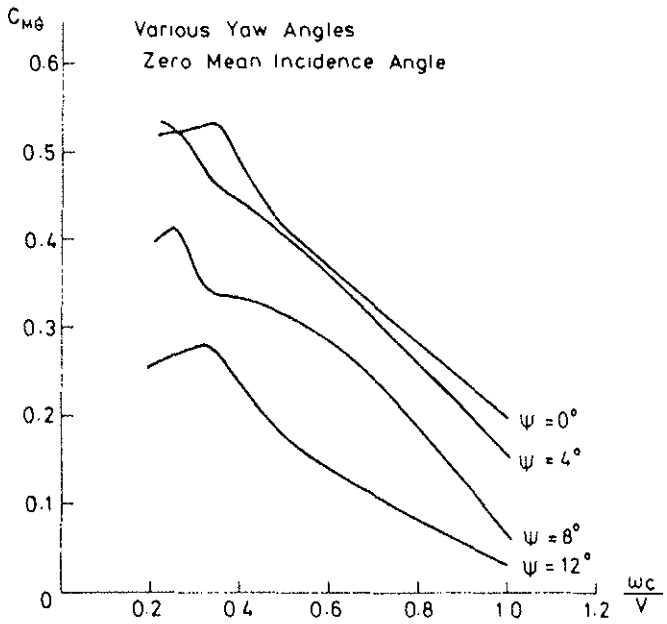

FIGURE 11 VARIATION OF $C_{M\dot{\theta}}$ WITH FREQUENCY PARAMETER

It must be remembered that because of the symmetry of a rectangular container about two of its axes, pitching and yawing derivatives are interchangeable.

The aerodynamic reactions of the container were then used to obtain the underslung load aerodynamic forcing functions for the right hand side of the equations of motion. These forcing functions - or stability derivatives - show the variation of the aerodynamic reactions for small perturbations of the underslung load. The calculation of these stability derivatives in contained in Reference 16.

6. COMPLETE EQUATIONS OF MOTION

The complete equations of motion are obtained by equating the inertia forces to the external forcing functions which cause the acceleration terms in the first place. These equations separate into mutually independent longitudinal and lateral sets, and are shown in figures 12, 13. Equations for the Sea King were for the case of zero initial pitch attitude and small steady state vertical velocity.

It must be remembered that for small perturbations $p = \dot{\phi}$, $q = \dot{\theta}$, $r = \dot{\psi}$, and that $\beta_2 = k\, \rho_2$ (k = .255 for 4.57 m, 15 ft suspension spread).

Combined Helicopter-Underslung Load X-Force Equation

$$(m_H + m_L)(\dot{u} + qw_0) + m_L\left[\ddot{\rho}_2 (c\cos\delta_0 + k\, z_G\cos\delta_0) + \dot{q}\, R_{2G0}\right]$$
$$+ v(X_u + X_{Lu}) + w(X_w + X_{Lw}) + q(X_q + X_{Lq})$$
$$- \theta\,(m_H + m_L)g + a_{1s}\, X_{a1s} + B_1\, X_{B1} + \dot{\rho}_2 X_{L\dot{\rho}2} + \rho_2\, X_{L\rho 2}$$

a_{1s} and B_1 are the rotor disc and autostabiliser terms respectively.

Combined Z-force Equation

$$(m_H + m_L)(\dot{w} - qu_0) - m_L\left[\ddot{\rho}_2 (c\sin\delta_0 + k\, z_G\sin\delta_0) + \dot{q}\, R_{XG0}\right]$$
$$+ u(Z_u + Z_{Lu}) + w(Z_w + Z_{Lw}) + q(Z_q + Z_{Lq}) + a_{1s}\, Z_{a1s} + B_1 Z_{B1}$$
$$+ \dot{\rho}_2\, Z_{L\dot{\rho}2} + \rho_2\, Z_{L\rho 2}$$

Helicopter Pitching Moment Equation

$$\dot{q}B = u\, M_u + w\, M_w + q\, M_q + a_{1s}\, M_{a1s} + B_1\, M_{B1} + \rho_2\sigma_H$$

The term $\rho_2\sigma_H$ is the interaction pitching moment.

Load Moments about Helicopter Pitching Axis

$$\dot{q}\, B_{L\dot{q}} + \dot{u}\, B_{L\dot{u}} + \dot{w}\, B_{L\dot{w}} + \ddot{\rho}_2\, B_{L\dot{\rho}2} + q\, B_{Lq} + \dot{w}\, M_{L\dot{w}} + \dot{q}\, M_{L\dot{q}}$$
$$+ \ddot{\rho}_2\, M_{L\dot{\rho}2} + u\, M_{Lu} + w\, M_{Lw} + q\, M_{Lq} + \dot{\rho}_2\, M_{L\dot{\rho}2} + \theta\, M_{LG\theta}$$
$$+ \rho_2(M_{LG\rho 2} + M_{L\rho 2} - \sigma_H)$$

Rotor Disc Fore-and-Aft Perturbations

$$\dot{a}_{1s} = u\, H_{fu} + w\, H_{fw} + q\, H_{fq} + a_{1s}\, H_{fa1s} + B_1\, H_{fB1}$$

Pitch Autostabiliser Law

$$\dot{B}_1 = -14.286\, B_1 + 10.214\theta + 7.143\theta$$

FIGURE 12 COMPLETE LONGITUDINAL EQUATIONS OF MOTION

Combined Sideforce Equation

$$(m_H + m_L)(\dot{v} + ru_0 - pw_0) + m_L\left[-\ddot{\rho}_1(c\cos\delta_0 + z_G\cos\delta_0)\right.$$
$$\left. + \dot{r}\, R_{XG0} - \dot{p}\, R_{ZG0}\right]$$
$$+ v(Y_v + Y_{Lv}) + p(Y_p + Y_{Lp}) + r(Y_r + Y_{Lr}) + \dot{\rho}_1 Y_{L\dot{\rho}1} + g(m_H + m_L)\phi$$
$$+ \rho_3\, Y_{L\rho 3} + b_{1s}\, Y_{b1s} + A_1 Y_{A1} + \sigma_t\, Y_{\sigma t}$$

In the equation above the terms b_{1s}, A_1 and σ_t are the rotor disc, roll autostab and yaw autostab perturbations.

Helicopter Rolling Moment Equation

$$\dot{A}\dot{p} = vL_v + pL_p + rL_r + b_{1s}\, L_{b1s} + A_1\, L_{A1} + \theta_t\, L_{\sigma t} + \rho_1 L_L$$

where $\rho_1 L_L$ is the helicopter-load interaction rolling moment.

Helicopter Yawing Moment Equation

$$C\dot{r} = vN_v + pN_p + rN_r + \theta_t N_{\sigma t} + \rho_3 N$$

where $\rho_3 v_N$ is the helicopter-load interaction yawing moment.

Load Moments about the Helicopter Rolling Axis

$$\dot{v}A_{L\dot{v}} + \dot{p}A_{L\dot{p}} + \dot{r}A_{L\dot{r}} + \ddot{\rho}_1 A_{L\dot{\rho}1} + \dot{\rho}_3 A_{L\dot{\rho}3} + pA_{Lp} + rA_{Lr}$$
$$= \dot{v}L_{L\dot{v}} + \dot{p}L_{L\dot{p}} + \dot{r}L_{L\dot{r}} + \ddot{\rho}_1 L_{L\dot{\rho}1} + vL_{Lv} + pL_{Lp} + rL_{Lr} + \dot{\rho}_1 L_{L\dot{\rho}1}$$
$$+ \dot{\rho}_3 L_{L\dot{\rho}3} + fL_{LG\phi} + vL_{LGv} + \rho_1(L_{LG\rho 1} + L_{L\rho 1} - \sigma_L) + \rho_3 L_{L\rho 3}$$

Load Moments about Helicopter Yawing Axis

$$\dot{v}C_{L\dot{v}} + \dot{p}C_{L\dot{p}} + \dot{r}C_{L\dot{r}} + \ddot{\rho}_1 C_{L\dot{\rho}1} + \dot{\rho}_3 C_{L\dot{\rho}3} + pC_{Lp} + rC_{Lr} = \dot{v}N_{L\dot{v}}$$
$$+ \dot{p}N_{L\dot{p}} + \dot{r}N_{L\dot{r}} + \ddot{\rho}_1 N_{L\dot{\rho}1} + vN_{Lv} + pN_{Lp} + rN_{Lr} + \dot{\rho}_1 N_{L\dot{\rho}1} + \dot{\rho}_3 N_{L\dot{\rho}3}$$
$$+ gN_{LG\phi} + vN_{LGv} + \rho_1(N_{LG\rho 1} + N_{L\rho 1}) + \rho_3(N_{L\rho 3} - \sigma_N)$$

Rotor Disc Equation

$$-\dot{b}_{1s} = vF_v + pF_p + b_{1s}\, F_{b1s} + A_1 F_{A1}$$

Roll Autostabiliser Law

The roll autostabiliser equation can be written as:

$$\dot{A}_1 = -100\, A_1 - 20\dot{\phi} - 13.2\phi$$

Yaw Autostabiliser Law

$$\dot{\theta}_t = .61\dot{r} + .16\dot{\phi} + .03\phi$$

where θ_t is change in the pitch of the tail rotor applied by the yaw autostabiliser.

FIGURE 13 COMPLETE LATERAL EQUATIONS OF MOTION

The fourteen equations presented in figures 12, 13 form two systems (longitudinal and lateral) of simultaneous differential equations; these equations have been linearise for small perturbations about the mean equilibrium position.

To examine for stability the characteristic equation is formed and solved to give the roots (or modes), which for a general case may be assumed to be complex. A root with a positive real part implies divergence, and hence instability, of motion in that mode. Eigenvectors (or modeshapes) are obtained for each root to identify the dominant degrees of freedom in that mode.

Stability analysis involves three steps. The motion of the helicopter is analysed first of all to determine its behaviour. Next the motion of the load alone can be obtained by ignoring all the helicopter perturbation variables, which is equivalent to the wind tunnel studies of an underslung load. These analyses for the helicopter and load in isolation may be regarded as establishing the reference solutions, when there are no mutual interaction effects. Finally motion of the combined helicopter-underslung load system is analysed. Comparison of these results with the first two stages gives the dynamic effects of the underslung load on the helicopter and vice versa.

7. ANALYSIS OF LONGITUDINAL EQUATIONS

Results from analysis of the longitudinal equations given in figure 12 are plotted in figures 14, 15, 16 showing the variation with airspeed of the real and imaginary parts of the roots of the characteristic equation.

7.1 Longitudinal Dynamics of the Sea King Helicopter

The variation with airspeed of the roots of pitch stabilised Sea King helicopter are shown in figure 14. MODE 1 is a very rapid subsidence in the longitudinal cyclic applied by the pitch autostabiliser, and the resulting response of the rotor disc.

MODE 2 is a heavily damped oscillation in the fore-and-aft perturbations of the rotor disc, with significant response in B_1 and w.

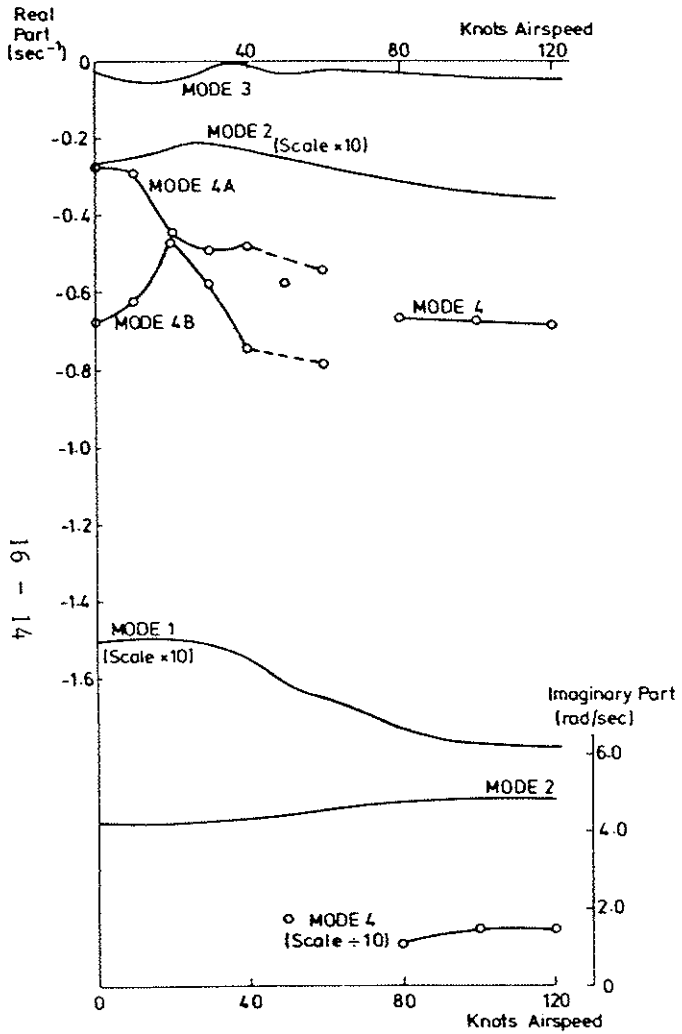

FIGURE 14 LONGITUDINAL MODES OF STABILISED SEA KING HELICOPTER

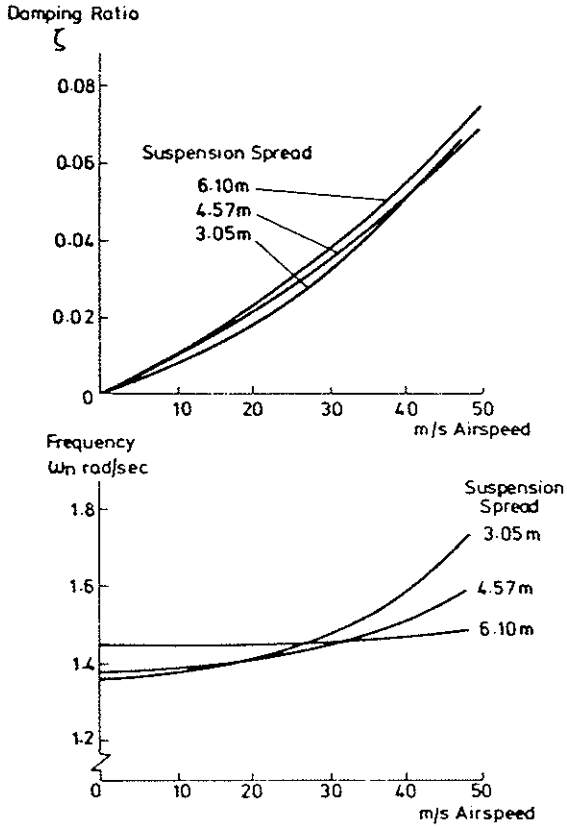

FIGURE 15 VARIATION OF DAMPING AND FREQUENCY FOR LONGITUDINAL MOTION OF LOAD

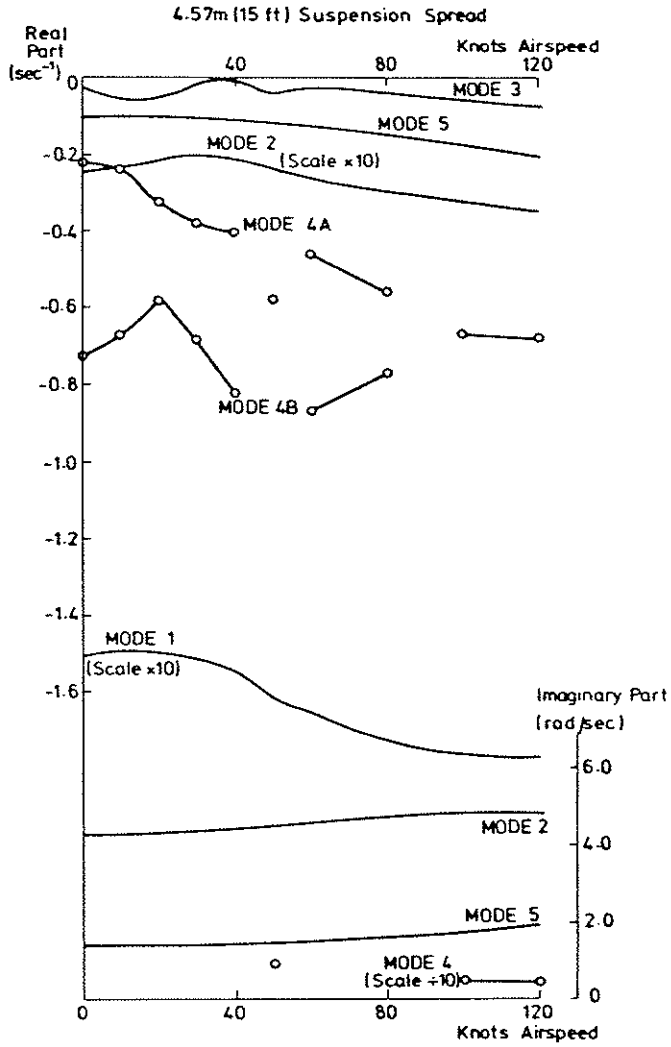

FIGURE 16 COMBINED LONGITUDINAL MODES STABILISED HELICOPTER

The remaining modes are mainly helicopter rigid body modes eg MODE 3 is a subsidence in u, the forward speed perturbations of the helicopter.

Modes, 4A and 4B, behave irregularly. They start off as two subsidences, the smaller in w and the larger, Mode 4B, in θ. The modal vector of the θ subsidence changes so that it too is a w mode at 20 kts and above. The two real roots combine to give a damped, low frequency oscillation in w at 50 kts and again at airspeeds greater than 80 kts.

7.2 Longitudinal Motion of the Load

Ignoring the helicopter degrees of freedom in the combined longitudinal equations presented above, a simple second order system is obtained, whose stability is governed by the damping term. Evaluating this term shows that the largest contribution is from the drag of the load. Thus although the pitch rate component is destabilising it is swamped by the load drag resulting in a damped oscillation.

The variation of damping and frequency are shown in figure 15 for three suspension spreads of 3.05, 4.57, 6.10 m (10, 15, 20 ft). The differences in the damping and frequency plots for the three spreads are quite small.

7.3 Combined Longitudinal Stability

Results from the longitudinal analysis of the combined system are shown in figure 16 for a 4.57 m suspension spread. MODES 1 and 2, which are the roots of the autostabiliser - rotor disc are unchanged from figure 14. The corresponding mode shapes are changed only by the presence of a small ρ_2 term.

Magnitude of MODE 3, subsidence in u the forward speed perturbations of the helicopter, is increased slightly as a direct consequence of the underslung load.

Greatest effect of the load is on Modes 4A and 4B, which are pushed apart so that the magnitude of the roots forming Mode 4A is reduced, while 4B is increased. Modal vectors show Mode 4A to be a vertical damping mode; Mode 4B starts off as a θ subsidence changing at 20 kts to another w root, as for the helicopter alone. These two modes combine to give an oscillation at 50 kts and at 100, 120 kts. Frequency of this oscillation, given by the imaginary part, is much reduced compared to the helicopter alone case.

The fore-and-aft motion of the load, MODE 5, is seen to be affected quite significantly by the helicopter. The damping plot shows roughly the same shape and the same change in magnitude as for the load alone except that the value at hover is .1 instead of zero (figure 15). The frequency is increased marginally.

8. ANALYSIS OF THE LATERAL EQUATIONS

It is the normal procedure to use only the roll channel of the lateral autostabilising equipment while carrying underslung loads. Results for the Sea King lateral dynamics with roll autostabiliser only are shown in figure 17, followed by load lateral analysis (figure 18), and combined analysis (figure 19).

8.1 Dynamics of Roll Stabilised Sea King Helicopter

Lack of the heading hold of the helicopter leads to a zero root in ψ the yaw perturbations of the helicopter, labelled as MODE 1 in figure 17. MODE 2 is the lateral cyclic applied by the roll autostabiliser, given by $\lambda = -100$.

MODE 3 starts off at hover as two real roots, which are yaw damping modes with negligible response from the remaining degrees of freedom. At 30 knots and above the two real roots combine to give a low frequency low damping oscillatory mode. The modeshape shows that at 30 kts there is an equal response in yaw and in sideslip velocity v. As speed increases the sideslip term becomes more significant with others decreasing relatively.

MODE 4 is a high frequency, high damping mode in the lateral perturbations of the rotor disc. The oscillation breaks up into two real roots at 120 kts: the smaller root is a convergence of the aircraft bank angle and the larger root is in the lateral rotor disc perturbations.

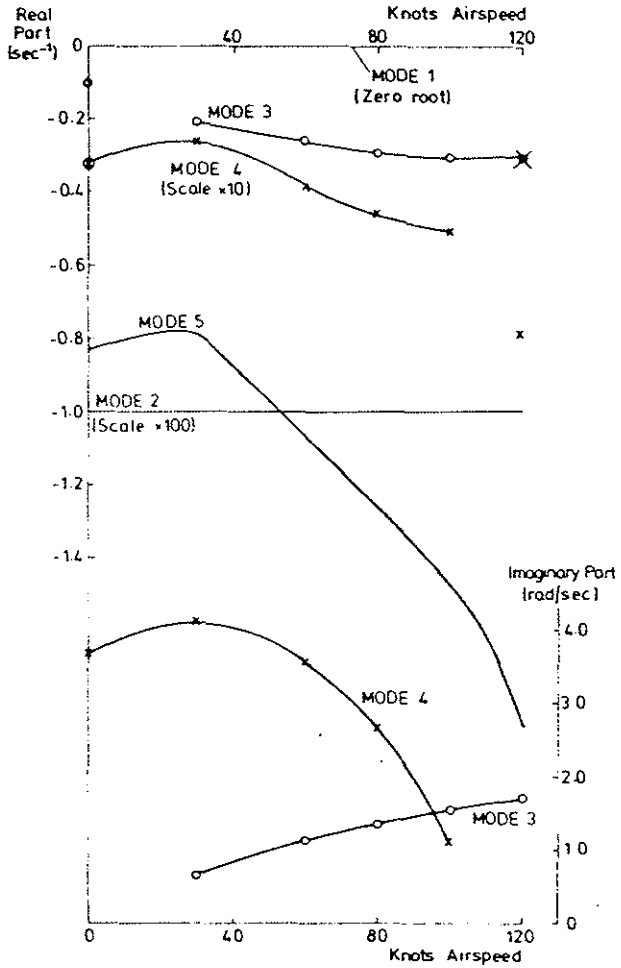

FIGURE 17 LATERAL ROOTS - SEA KING HELICOPTER WITH ROLL AUTOSTABILISER

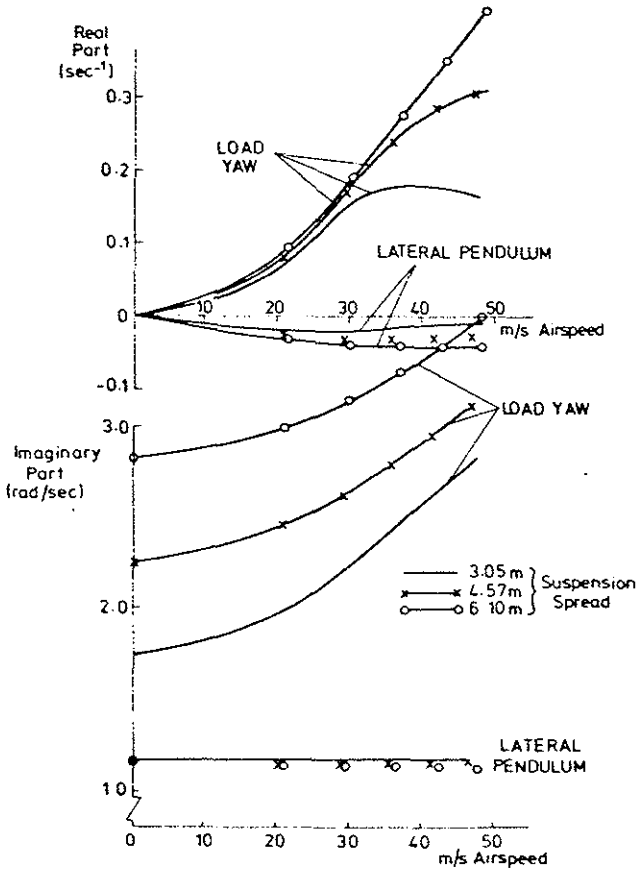

FIGURE 18 LATERAL DYNAMICS OF UNDERSLUNG LOAD

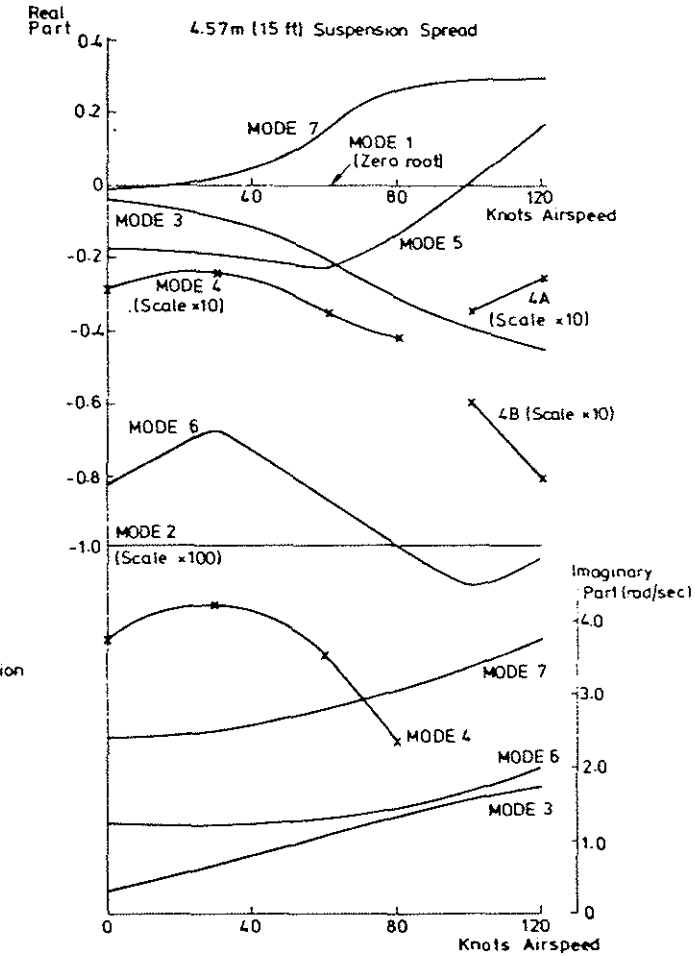

FIGURE 19 COMBINED LATERAL STABILITY, ROLL STABILISED HELICOPTER

MODE 5 is a real negative root. The modeshape shows this root to be a roll convergence, with large responses in v and ψ at hover. As the speed is increased the mode becomes more strongly a roll convergence.

8.2 Lateral Motion of the Load

A two degree of freedom system is obtained for the lateral dynamics of a rectangular container slung by four cables from two longitudinally separated suspension points. The solution yields two pairs of complex conjugate roots which give two oscillatory modes - one in load yaw and the other in load lateral motion.

Results presented in figure 18 are for the load suspended from spreads of 3.05, 4.57, 6.10 m (10, 15, 20 ft). It is seen that the yaw mode has a positive real part, indicating an unstable, exponentially increasing oscillation. The load is most unstable when suspended from a 6.10 m spread. The frequency of yaw oscillation is strongly influenced by the suspension spread because the yaw stiffness increases as the spread is increased. The frequency also increases with increasing airspeed.

The lateral pendulum mode is damped, though only very slightly, at all speeds. The exponential damping factor increases in magnitude as the spread is increased. The frequency of the lateral pendulum mode decreases very slightly as the suspension spread is increased.

The mode shapes obtained for the level flight case indicate little cross-coupling between the two normal coordinates (ρ_1 and ρ_3) of the lateral motion of the load; as the suspension spread increases the coupling between the two modes decreases.

8.3 Combined Lateral Stability

Full results for the combined lateral stability are discussed in Reference 23. Results from the lateral stability analysis of a roll stabilised helicopter carrying an underslung load from a 4.57 m suspension spread are plotted in figure 19.

MODEs 1 and 2, the zero heading hold of the helicopter, and the lateral cyclic applied by the roll autostabiliser, are unchanged from figure 17.

MODE 3 is an oscillation at all speeds now. Frequency variation is the same as in figure 17, while the real part is increased in magnitude resulting in increased damping. The modal vector shows that as for the helicopter alone, the dominant degree of freedom changes from ψ to v. This however excites a substantial response of the load lateral motion.

MODE 4 is shown as an oscillation only up to 80 kts (compared to 100 kts for the helicopter alone). The damping of the oscillation is slightly less, and frequency greater, than for the helicopter alone. The modal vector shows that as for the helicopter alone the largest term is b_{1s} and ϕ. There is however a large contribution (greater than ϕ) from ρ_1, the load lateral motion.

Mode 4 breaks up into two real roots at 100, 120 kts. The smaller root, Mode 4A, is a convergence in the helicopter bank angle, with large b_{1s} and ρ_3 terms. The load yaw contribution ρ_3 increases as the speed is increased. The larger root is a subsidenc in the rotor disc lateral motion.

MODE 5 is changed completely by the presence of the underslung load as the mode, instead of becoming a stronger subsidence, turns into a divergence. The modal vector is also changed so that virtually the only response at hover is in ψ. At 30 kts a large ρ_1 term appears which then dominates the modeshape up to 120 kts. A load yaw ρ_3 term also appears and increases slowly with airspeed. Thus this mode is changed from a helicopter roll subsidence to a load lateral divergence.

MODE 6 is the load lateral pendulum mode. The helicopter has a strong effect on this mode as the damping, given by the negative real part, is increased considerably and the frequency nearly doubled compared to the load alone case of figure 18. The largest term is ρ_1 at all airspeeds; this seems to excite an increasing response in helicopter sideslip.

The load yawing oscillation, labelled MODE 7, is marginally stable at hover but becomes unstable as the speed is increased. Frequency is increased slightly compared to the load alone case.

9. CONCLUSIONS

Following conclusions can be drawn from the results presented in this paper:

a. Wind tunnel tests on an oscillating model of the rectangular container show significant moment terms due to pitch rate.

b. Analysis of the equations of motion of the underslung load alone shows that fore-and-aft oscillation and lateral pendulum mode are damped, but the yawing oscillation is divergent.

c. Longitudinal studies of the combined helicopter-underslung load equations show little effect of load on the helicopter.

d. Slinging the load beneath the helicopter increases the frequency of fore-and-aft oscillation slightly and the damping is made much higher.

e. Studies of the combined helicopter-underslung load lateral equations of motion show a stronger effect of the load on the helicopter. The effect is generally destabilising as the damping of most of the helicopter modes is reduced.

f. The helicopter has a beneficial effect on the lateral load dynamics. Damping of the lateral pendulum mode is increased considerably while the yawing motion is marginally damped at low airspeeds.

g. Studies of the combined lateral equations show strong coupling between helicopter sideslip velocity and load lateral motion.

h. Effect of the roll stabilised helicopter on the load dynamics suggests that a possible technique for stabilising the load is to suitably change the roll autostabiliser law.

REFERENCES

1. Lucassen L R; Sterk F J. "Dynamic Stability Analysis of a helicopter with a sling load", J of American Helicopter Society, Vol 10, No 2 April 1965

2. Wolkovitch J; Johnston D E. "Automatic control considerations for helicopters and VTOL aircraft with and without sling loads". Systems Technology Inc., Technical Report No 138-1, November 1965.

3. Wolkovitch J; Peters R A; Johnston D E. "Lateral control of hovering helicopter with and without sling loads", STI Technical Report No 145-1, May 1966.

4. Gabel R; Wilson G J. "Test approaches to external sling load instabilities", J American Helicopter Society 15(3), July 1968.

5. Wilding J M D. "A report on experimental external load carrying with WS55 and S61 helicopters", BEA Helicopters Ltd, HL/PD/TR/61/55/85, February 1969.

6. Opatowski T. "Load lifting with helicopters: A resume of A & AEE experience and other considerations", A & AEE, Boscombe Down, November 1969.

7. Staley J A; Sankewitsch V. "Sling load yaw instability speeds in AHH Flight Demonstration Hardware Tests", Boeing Vertol IOM 8-7453-1-1845, May 1969

8. Sheldon D F. "A study of the stability of a plate like load towed beneath a helicopter", PhD Thesis, University of Bristol, 1968.

9. Abzug M J. "Dynamics and control of helicopters with two-cable sling loads", AIAA Paper No 70-929, July 1970.

10. Wilson G J; Rothman N N. "Evaluation, development and advantages of the helicopter tandem dual hook system," AGARD CP-121, Sept 1971.

11. Dukes T A. "Manoeuvring heavy sling loads near hover", 28th National Forum of the American Helicopter Society, Preprint No 630 May 1972.

12. Asseo S J; Whitbeck R F. "Control requirements for sling-load stabilisation in heavy lift helicopters", J of American Helicopter Society, July 1973.

13. Wilding J M D. "The helicopter as an aerial crane", Royal Aeronautical Society Lecture to Swindon Branch, April 1974.

14. Sheldon D F. "An appreciation of the dynamic problems associated with external transportation of loads from helicopters - state of the art", 1st European Rotorcraft and Powered Lift Aircraft Forum, University of Southampton, September 1975.

15. Poli C; Cromack D. "Dynamics of slung bodies using a single point suspension", J Aircraft, February 1973.

16. Prabhakar A. "A study of the effects of an underslung load on the dynamic stability of a helicopter", PhD Thesis, Royal Military College of Science, Shrivenham, 1976.

17. Zajac A. Basic Principles and Laws of Mechanics, D C Heath & Co, NY 1966.

18. Sheldon D F; Pryor J. "Phase 5 - The Aerodynamic characteristics of various rectangular box and closed cylinder loads", Technical Note AM/41, Royal Military College of Science, April 1973.

19. Frazer R A; Duncan W J; Collar A R. Elementary Matrices, Cambridge University Press 1963.

20. Babister A W. Aircraft Stability and Control, Pergamon Press 1961.

21. Prabhakar A; Sheldon D F. "Wind tunnel tests to determine the oscillatory derivatives of a rectangular container", Technical Note No AM/58, Royal Military College of Science, July 1974.

22. Prabhakar A; Sheldon D F. "Dynamic Stability of a helicopter carrying an underslung load", Technical Note AM/78, Royal Military College of Science, August 1976.

23. Prabhakar A. "Lateral dynamic stability of a Sea King helicopter carrying an underslung rectangular cargo container", Technical Note MAT/7, Royal Military College of Science, June 1977.